Study of a laminar falling film flowing over a wavy wall column: Part II. Experimental validation of hydrodynamic model

S. Negny, M. Meyer *, M. Prevost

UMR 5503 INP-ENSIGC/CNRS, Groupe Séparation Gaz-Liquide, 18 Chemin de la Loge, 31 078 Toulouse Cedex 04, France

Abstract

The interface position of a film flowing over a wavy wall column is experimentally studied by an optical method composed of a charge coupled device (CCD) video camera. The results are compared with theoretical calculations and show a good agreement between results for both the film thickness and the vortex position. However, there exist some discrepancies because the interface is travelled by waves not accounted for in the mathematical model as it is supposed to be flat. Some characteristics of the waves are experimentally noted. Furthermore, the influence of the viscosity on the film thickness is established as well.

1. Introduction

The film flow is translated by a liquid falling down under gravity effect with one free boundary, i.e. the interface. The flow of a liquid alone or combined with a gas is frequently studied and used in chemical engineering. This gravitational flow of a liquid has been essentially studied using smooth solid surfaces. We have decided to use a wavy surface as this kind of surface offers a particular flow pattern in the case of full channel [1]. We have studied the hydrodynamics of this type of wall for the film in order to understand the influence of the flow behaviour on the transfer process.

The local thickness of the film is one of the principle parameters that need to be determined and certainly the most complicated one, owing to the presence of ripples over the film interface. There are various methods for determining the interface profile: the capacity method with two needles (Chu and Duckler [2], Takahama and Kato [3] and a better version by Leuthner et al. [4]), as well as the capacity method with one needle (Lyu and Mudawar [5]). The principle drawback of these methods is the calibration which is very long and scrupulous.

Furthermore, with this technique, the needles are immersed in the liquid therefore they disturb the film flow (even if the needles used are thinner and thinner; 50 μm for Leuthner et al. [4]). Another drawback is that this method cannot be used in the case of evaporation and condensation when there is no flow rate. Another way to reach the interface profile is to use an optical method like the scattering light method (Salazar and Marschall [6]). The inconvenience of this method is that it is very expensive. Further details and others methods are explained by Alekseenko et al. [7].

In our case, the falling film flows over a wavy wall surface, the scattering light method is therefore impossible to use as the laser beam must be oriented perpendicularly to the wall and our wall shape complicates this experimental requirement. Our problem is solved by use of an optical method composed of a video camera. The first part of this paper is dedicated to the description of the experimental apparatus and procedure. In the second part calculations and experiments are compared, as a theoretical investigation has already been carried for the falling film with a free interface flowing over a wavy wall surface, as previously described by Negny et al. [8]. The particularity of this model resides in the flow field which contains a mobile gas liquid interface without ripples. The interface position is determined by an equation based on a force balance [9]. This analysis

---

* Corresponding author.
E-mail address: Michel.Meyer@ensigct.fr (M. Meyer).

postulates laminar steady flow range, because it is very difficult to treat turbulent flow with a free interface and separation of the flow. The flow behaviour is characterised by the Navier Stokes equations expressed in terms of stream function and vorticity. As the periodicity of the wall shape, the model is reduced to one wave of the solid surface. Another important assumption is that the gas phase is supposed to be stagnant and it is not accounted for in the theoretical model.

2. Experimental apparatus and procedure

2.1. Apparatus

For the laminar flow, we have observed the interface position and measured the film thickness over a wavy wall column. The experimental apparatus is a closed hydrodynamic loop, schematically shown in Fig. 1. The test fluid used for all experiments was distilled water except when the viscosity effects were evaluated. Water is pumped into the receiving tank (5), with a centrifugal pump (1). The fluid temperature is kept constant at 293 K by a controlled electrical pre-heater (2) in order to have constant fluid properties like in the case of the theoretical calculation. The flow rate is determined with a flowmeter and controlled by a flow valve (3). The fluid is driven to the inlet of the test section (4). The fluid flows over the outside of the column. At the bottom of the column, the liquid returns to the receiving tank.

The test section is composed of sinusoidal wavy column with a constant wall shape. The column was made in a single piece of aluminium covered by a black facing settled by an anodic oxidation. The fluid does not
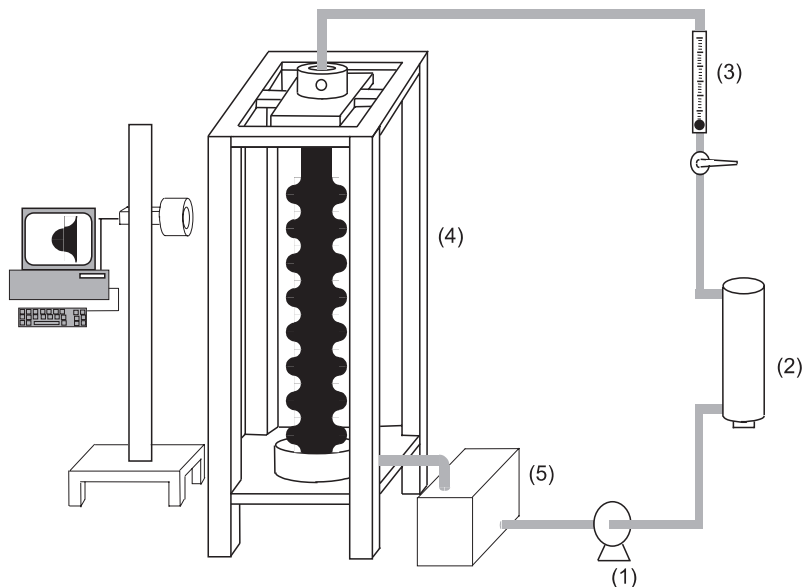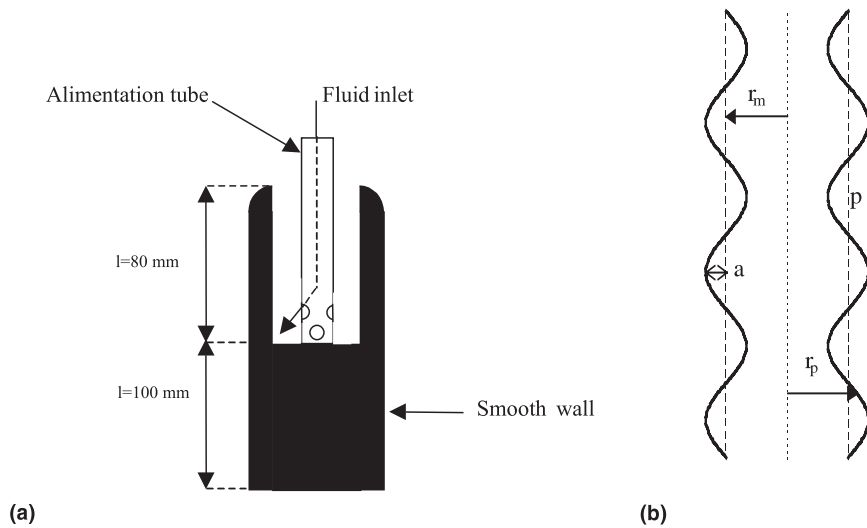

Fig. 1. Experimental apparatus.

Fig. 2. (a) Fluid inlet at the head of the column; (b) geometric definition of the waves.

flow directly over the wavy surface but over a 0.185 m long smooth surface in order for it to stabilise. Fig. 2(a) details the fluid inlet. The fluid inlet was fed by overflow and the exterior of the ridge is rounded in order to avoid flow perturbation. After this smooth part, the fluid flowed over the wavy surface composed of 31 furrows, each furrow is 22 mm long (p), 8 mm deep ($2a$) and the column mean radius is 20 mm (r_m). The column is 0.91 m long and the wavy wall surface is about 0.73 m long. Fig. 2(b) gives the details of the geometric characteristics of the wall. The measurements were undertaken for the laminar flow range for $Re = 4\Gamma/\mu \leqslant 300$. The column is protected from gas circulation.

A very important point is that the column must be vertical to avoid consequential effects on the flow pattern (for example: creation of an angular velocity) and to obtain a circumferential uniformity of the flow. There are two systems to ensure the verticality. The first is located at the back of the column and permits a rough two directional adjustment. The second system is established to refine the adjustment at the head of the column. The adjustment is realised by a catetometer, which is an optical apparatus composed of a line of sight which permits to precisely adjust the tube.

2.2. Procedure

To appraise the film thickness an optical method is used. The optical apparatus is composed of a matricial charge coupled device (CCD) video camera connected to an image treatment software package: Optilab. This software package was conceived to answer to scientific and industrial requirements. It gives a complete range of functions for the treatment, analysis and interpretation of shots. Its capacities allow us to accomplish various

work and studies. During measurements, the camera is fixed at a distance from the inlet nevertheless the camera is able to move all along the column.

The CCD camera and Optilab shot the contrast between two objects. In order to have the best possible contrast the column is black and the wall behind was painted white. The video camera is adjusted in order to have one furrow on the wall on the shot. The experimental procedure consists of three steps. Firstly, we shoot an image of the column without the liquid film and the shot is treated to increase the contrast (Fig. 3(a)). In the second step, we shoot an image, Fig. 3(b), with the liquid film. This shot is treated for the same reason as before. Between the first two steps the camera must stay at the same place owing to the treatment of the third
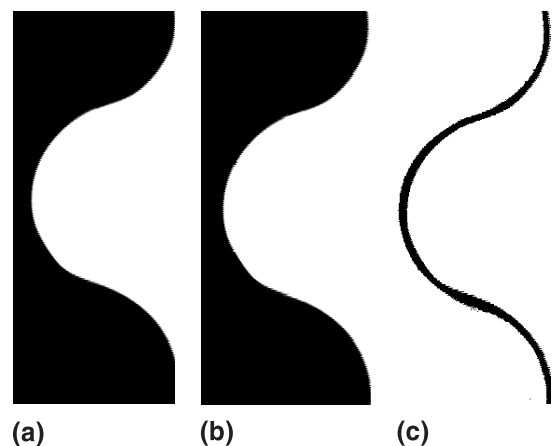

Fig. 3. Three successive steps for film visualisation: (a) wavy surface; (b) wavy surface and film; (c) film.

step. The last step, Fig. 3(c), consists in the removal of the first shot from the second for measuring the film thickness as after treatment, only the pixels not common to the two first shots are visible on the third one. These pixels correspond to the film. On the final shot, the measurement of the film thickness is very precise because each pixel represents 3×10^{-3} mm^2 of the photographed object. Three shots are taken for each thickness measurement.

3. Results and discussion

Before starting the experiments, some characteristics of the flow have been controlled. The verticality has been the first subject of preoccupation. For a furrow, the film thickness is measured at different angular positions. The furrow chosen (27th) is far from the entrance and the flow rate is important (30 l/h) because if a default exists in the verticality, it is amplified at a high flow rate and clearly visible at the end of the column. The film interface profile is the same for each angular position, this ensures a correct adjustment of verticality. The second characteristic studied is the minimum flow rate for which the column is not totally wet by the liquid film. When we start with a high flow rate and we decrease it, the first dry zone appears for a flow rate of 5 l/h which corresponds to $Re = 43.8$. Even if the column is covered by a black facing, the minimum flow rate is very low.
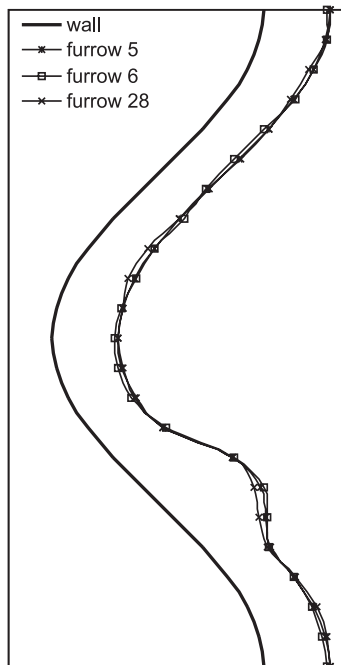
The last point concerns the periodicity. In the theoretical description of the flow, periodical conditions are expressed for one wave profile. Even if this condition is true for a flow inside a full channel, it needs to be verified for the film. The periodicity is translated by the same film thickness at the beginning and the end of the wave. This film characteristic is obtained for all the Reynolds numbers of the laminar flow range. Another way to validate this condition is to compare the interface film profile for different furrows. An example of results obtained at $Re = 200$ are presented on Fig. 4. Here again, the interface profile is the same for each wave of the column (except for the entrance region) and for all Reynolds numbers. As a conclusion the assumption of periodicity is realistic for the laminar flow.

3.1. Flow pattern

The calculated stream lines for the same wall geometry as the experimental column are expressed for various Reynolds numbers in a previous paper by Negny [9]. Experimentally, the vortex is always present because the minimum flow rate corresponds to $Re = 43.8$, but the vortex numerically arises at $Re = 15$ for this geometry.

Now we shall explain the vortex formation. In the case of a flow, the influence of the viscosity is located in a thin layer (boundary layer) near the solid surface. For a flow without friction, i.e. outside the boundary layer, the fluid particles are accelerated from A to B and decelerated from B to C, as noted in Fig. 5. As a consequence, the pressure decreases from A to B and increases from B to C. A particle inside the boundary layer is under the influence of the same pressure field. The particle looses a great part of its kinetic energy to counter the friction forces on A and B. At B, its kinetic energy is not strong enough to win the pressure gradient between
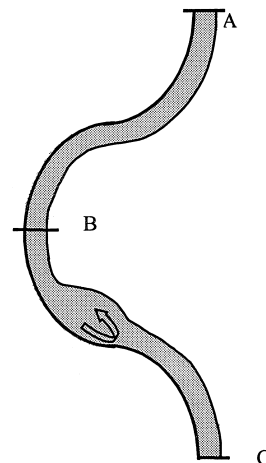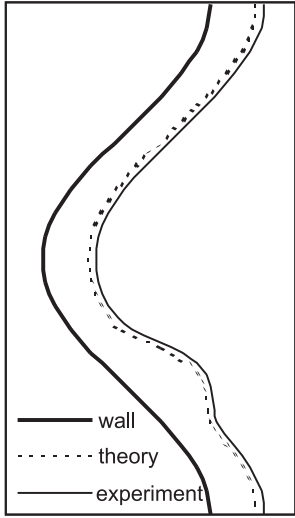

Fig. 4. Verification of the periodicity: example $Re = 200$.

Fig. 5. Vortex formation.

Fig. 6. Comparison of the interface position for $Re = 150$.

Fig. 7. Ratio of mean thickness in the region without recirculation.

Fig. 8. Ratio of the maximum mean thickness.

B and C. This, the pressure gradient imposes a change of flow direction to the particle and the vortex arises as a consequence.

The comparison of calculated and observed interface position is stated for the steady flow, far from the entrance region. This region is characterised by an increase of the film thickness and it concerns one furrow for a Reynolds number less than 150, two furrows for a Reynolds number between 150 and 250, and finally three furrows for the end of the laminar regime ($Re = 300$). The comparison at $Re = 150$ is shown in Fig. 6. Both results are in good agreement on the interface profile. The above calculations and experiments indicate two regions. One from the beginning to the middle of the furrow where the film thickness is constant. On the second part of the furrow, the film becomes thicker at the vortex location. After the vortex, the film thickness takes its initial value, i.e. value of the beginning of the furrow. This agreement validates the specific equation used in the modelling part for describing the interface position.

In order to detail the comparison, Figs. 7 and 8, respectively represent the ratios between experimental and theoretical mean thickness in the region without recirculation (i.e. where the thickness is constant) and the maximal mean thickness at the vortex location. Both figures are quite similar and we can see a good agreement between experiments and calculations because ratios are near to one. Nevertheless, there are two important differences. First of all, after $Re = 300$ the ratios greatly increase. The reason for this is that although the experimental flow pattern becomes unsteady and turbulent at a Reynolds number above 300, theory considers 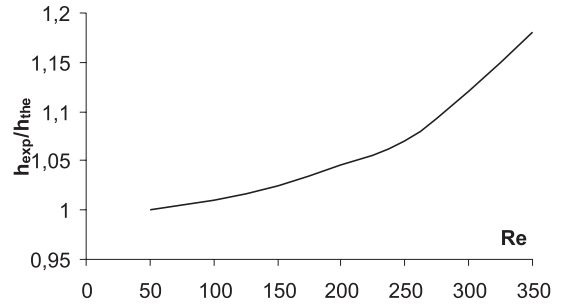a steady laminar flow. Secondly, th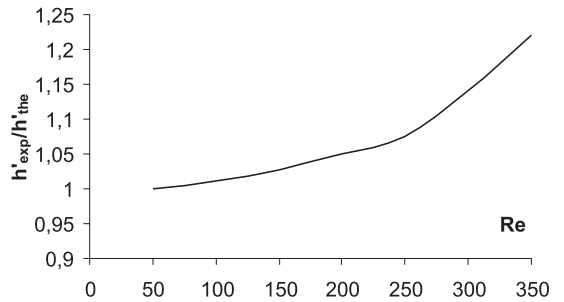e ratios are always greater than one, especially for a Reynolds number greater than 150. For this regime, we experimentally discover the presence of micro waves over the interface. The waves increase the experimental value of the thickness, taking into account the accuracy (1 pixel). With an increase of the Reynolds number, the wave amplitude is enhanced and so the ratios increase. For the model, the interface is supposed to be flat without ripples so this phenomenon is not accounted for (without this assumption, the specific interface equation cannot be reached).

Comparison of the vortex position is another way to validate the numerical results. The representation of the location of the vortex is translated by the position of two particular points, Fig. 9: the separation point (S points) where the flow starts to leave the wall and the reattachment point (R points) where the main stream reattaches itself to the wall. On this figure we can underline that the vortex size increases as the Reynolds number increases. Experimentally, the vortex seems to be centred at the same place but it goes further downstream (less than 2 mm) for a Reynolds number between 50 and 150 in the case of the theoretical results. Nevertheless, the model gives good results and the agreement is good for a Reynolds number greater than 150. This difference can be explained by the accuracy of the
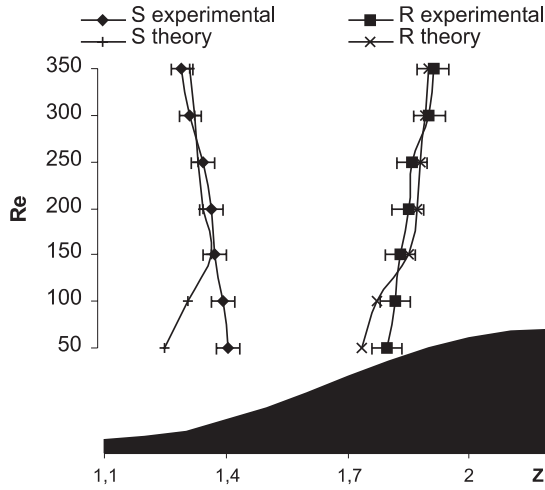
Fig. 9. Comparison of the vortex location.

experimental method for Reynolds numbers smaller than 150. For low Reynolds numbers, the film thickness is very low (less than 1 mm) and the increase of the thickness at the vortex location is not very important. As a consequence, the determination of the points where the thickness starts to grow and where it takes its initial value is very difficult. These positions are estimated with an error of two or three pixels which explains the difference. When the Reynolds number increases, the position is easily visible because the enhancement of the film thickness is clearer, this is why the difference decreases. The error on the position of the points is about 4.5% for $Re = 45$ and 1.7% for $Re = 300$.

In this Fig. 9, there is a second discrepancy between both results, the vortex size is always lower in the experimental case. This is due to the way of determining the separation and reattachment points. Experimentally, these points are respectively determined where the thickness starts to grow and takes its initial value. But at the numerical location of these points (where the flow leaves and reattaches the wall) the change of thickness is too small to be detected by the experimental measurement. As a consequence the separation point is experimentally detected further downstream and the reattachment upstream.

This good agreement on the vortex position is very important because it validates the velocity field (intensity of recirculation, value of the velocity) within the film. Effectively, if the vortex recirculates with a greater (respectively lower) velocity, the position of the separation point moves upstream (respectively downstream) and the position of the reattachment moves downstream (respectively upstream). Here we have the same vortex size and position (if we take into account the error of measurement), that ensures a correct value of the velocity inside the film.

3.2. The waves

The experimental study reveals that the interface is destabilised by intermittent waves. The method of measurement is not adapted for the study of waves, nevertheless their major characteristics can be extracted. For a correct measurement of the wave velocity, it is necessary to use another CCD video camera which is able to take sequential shots. With our experimental apparatus it is impossible to know the value of the frequencies of the waves and velocities but the waves' amplitude is visible on the shot. To start this study, the video camera is located on the fifth furrow in order to see the waves at the head of the column but in avoiding the specific hydrodynamic of the entrance region. Until $Re = 100$, the interface is flat, without ripples, Fig. 10. For $Re = 100$, there are small and fast instabilities on the interface, that cannot be detected by measurement. With a further increase of the Reynolds number, fast waves with a small maximum thickness appear over the interface. As the Reynolds number increases the wave maximum thickness increases but the wave velocity seems to decrease.

In Fig. 11, we can see the evolution of the waves maximum thickness, along the column. For all Reynolds numbers, the waves arise and evolve to constant wave maximum thickness. The greater the Reynolds number, the greater the wave maximum thickness and the faster the constant wave maximum thickness is reached. However for $Re = 300$ there is no evolution stage and the interface is very disturbed by the waves. This is due to the transition to turbulent flow.
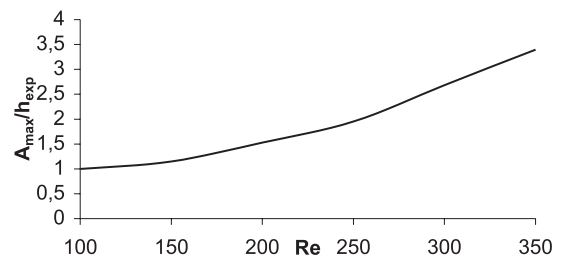

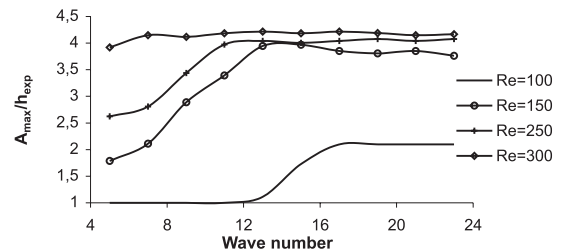Fig. 10. Maximum wave thickness on the fifth furrow.

Fig. 11. Maximum wave thickness along the column.

3.3. Viscosity

The influence of viscosity on the interface profile is studied with mixtures of water and glycerol which allow to have a wide range of viscosity, Table 1. With the change of viscosity the general profile of the interface is the same, i.e. constant thickness along the wave except at the vortex position where the film becomes thicker. Figs. 12 and 13, respectively, represent the mean constant thickness, and the mean maximum thickness for the vortex, for various flow rates. For a constant flow rate, when the viscosity decreases the mean constant thickness decreases too because the friction forces are less important, thus the boundary layer is thinner. About the mean maximum thickness, there is the same evolution because when the viscosity increases the boundary layer is enhanced, therefore the quantity of

Table 1
Viscosity of the mixture water–glycerol at 293 K

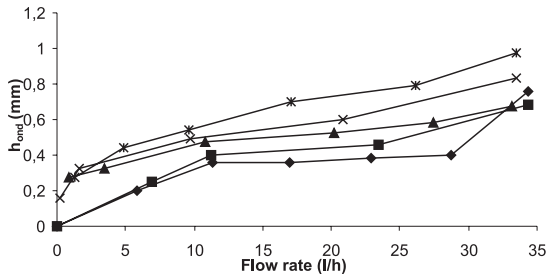| Mass fraction of glycerol	Viscosity (10^{-3} Pa s)
0	1
0.24	1.85
0.46	4.21
0.52	6.36
0.6	11

Fig. 12. Mean constant thickness for various viscosities ($\times 10^{-3}$ Pa s): (◆) 1; (■) 1.85; (▲) 4.21; (×) 6.3; (∗) 11.
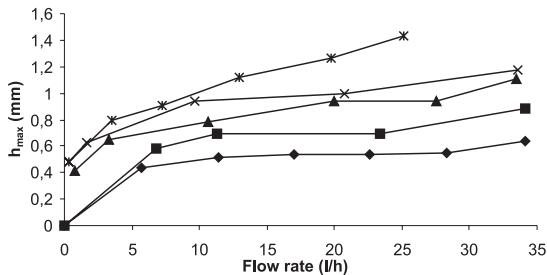

Fig. 13. Mean maximum thickness for various viscosities ($\times 10^{-3}$ Pa s): (◆) 1; (■) 1.85; (▲) 4.21; (×) 6.3; (∗) 11.

Table 2
Flow rates for the formation of the first wave

Viscosity (10^{-3} Pa s)	Flow rates (l/h)
1.85	13
6.36	16
11	23

fluid brought under recirculation is more important. The viscosity has an influence upon the formation of waves too. The flow rate for the formation of the first waves are in given Table 2. Finally, the waves appear for higher flow rates when the viscosity increases. This is due to important friction forces which keep the fluid on the wall and avoid wave formation. Another property affects the wave formation. With an enhancement of the film mass fraction of glycerol, the surface tension is increased too and it contributes to avoid the wave formation.

4. Conclusion

The flow characteristics of a falling film flowing over a wavy column were obtained experimentally and compared to theoretical results. The study concerns the laminar flow range which exists for Reynolds numbers smaller than 300 and a subsequent increase of this number causes turbulent flow with an unsteady vortex motion. During the laminar flow the vortex arises at $Re = 15$ (theoretically) and expands with Reynolds number and the film becomes thicker. Experimentally, the minimum Reynolds number studied is about 44, and the vortex is visible. At $Re = 150$ another phenomenon is highlighted: the formation of the wave over the interface. These waves increase in amplitude and decrease in velocity with an enhanced Reynolds number.

The relationship between viscosity and film thickness is also obtained. In the laminar flow, the film becomes thicker with viscosity because the friction forces are more important. Finally, the agreement is good between calculations and experiments. Meanwhile, two discrepancies appear

- The model does not predict the transition to the turbulent flow because it is developed for the steady flow.
- The waves are not present over the theoretical interface owing to the assumption that no ripples occur.

The particular flow pattern of the film flowing over a wavy wall can be used in heat and mass transfer operations. The vortex cuts off the thermal boundary layer developing at the wall vicinity, an enhancement of the heat transfer through the wall can also be predicted. In the theoretical model presented in the preceding paper, the mass transfer is underestimated for various reasons:

- The waves are not accounted for and they greatly enhance the mass transfer as we can see in studies concerning falling film flowing over a smooth surface.
- The gas phase is supposed to be stagnant, thus, there is no shear stress at the interface. This shear stress is beneficial for transfer. Furthermore with a flowing gas, a vortex can also develop in this phase, increasing the mass transfer to the interface.

Future preoccupations include introduction of the gas phase in the theoretical model and the simulation of. the film behaviour in the turbulent flow regime.

References

[1] T. Nishimura, Y. Ohory, Y. Kajimoto, Y. Kawamura, Flow characteristics in a channel with symmetric wavy wall for steady flow, J. Chem. Eng. Japan 17 (1984) 466–471.

[2] K.J. Chu, A.E. Dukler, Statistical characteristics of thin, wavy films: part II. Studies of the substrate and its wave structure, A.I.Ch.E. J. 20 (1974) 695–706.

[3] H. Takahama, S. Kato, Longitudinal flow characteristics of vertically falling liquid films without concurrent gas flow, Int. J. Multiphase Flow 6 (1980) 203–215.

[4] S. Leuthner, A.H. Maun, H. Auracher, A high frequency probe for wave structure identification of falling films, 3rd International Conference on Multiphase flow, ICMF'98, Lyon France, June, 1988, pp. 9–12.

[5] T.H. Lyu, I. Mudawar, Statistical investigation of the relationship between interfacial waviness and sensible heat transfer to a falling liquid film, Int. J. Heat Mass Transfer 34 (1991) 1451–1464.

[6] R.P. Salazar, E. Marschall, Time average local thickness measurement in falling liquid film flow, Int. J. Multiphase Flow 4 (1978) 405–421.

[7] S.V. Alekseenko, V.E. Nakoryakov, B.G. Pokusaev, Wave Flow of Liquid Films, Begell House, New York, 1994.

[8] S. Negny, M. Meyer, M. Prevost, Simulation of velocity fields in a falling film with a free interface flowing over a wavy surface, Computers Chem. Eng. 22 (1998) S921–S924.

[9] S. Negny, Modélisation et étude expérimentale d'un film liquide laminaire à interface libre ruisselant sur une surface structurée: couplage hydrodynamique – transferts de masse et énergie, PhD thesis, INP-ENSIGC, Toulouse, France, 1999.